

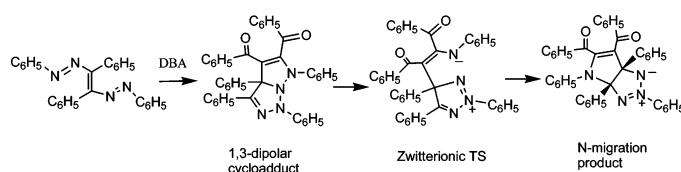
## Rearrangement of 1,3-Dipolar Cycloadducts Derived from Bis(phenylazo)stilbene: A DFT Level Mechanistic Investigation<sup>#</sup>

Cherumuttathu H. Suresh,<sup>\*,†</sup> Danaboyina Ramaiah,<sup>‡</sup> and Manapurathu V. George<sup>‡,§</sup>

Computational Modeling and Simulation Section, Photosciences and Photonics Section, Chemical Sciences and Technology Division, Regional Research Laboratory (CSIR), Trivandrum 695 019, India, and Jawaharlal Nehru Centre for Advanced Scientific Research, Bangalore 560 064, India

sureshch@gmail.com

Received August 17, 2006



The 1,3-dipolar cycloaddition of bis(phenylazo)stilbene with activated ethene and ethyne derivatives and the subsequent rearrangement of the cycloadducts have been studied using model compounds at the B3LYP/6-31G(d) level of density functional theory (DFT). From the structural and electronic features, a five-membered zwitterionic ring system **9** (1,2,3-triazolium-1-imide system) formed from bis(phenylazo)ethylene is confirmed as the active 1,3-dipole species in the reaction. Formation of the 1,3-dipolar cycloadduct from the alkyne derivative is found to be 26.0 kcal/mol exergonic, and it requires an activation free energy of 19.4 kcal/mol. The 1,3-cycloadduct formed in the reaction undergoes a very facile migration of a nitrogen-bearing fragment, passing through a zwitterionic transition state. A small activation free energy of 8.2 kcal/mol is observed for this step of the reaction, and it is 19.6 kcal/mol exergonic. Further activation of the newly formed rearranged product is possible under elevated temperatures, again passing through a zwitterionic transition state and resulting in the formation of 2,5-dihydro-1,2,3-triazine derivatives. Such derivatives have been recently reported by Butler et al. (*J. Org. Chem.* **2006**, *71*, 5679). The charge separation in **9** and the zwitterionic transition states are stabilized through the  $\pi$ -system of the phenyl rings and the carbonyl groups. Similar structural, electronic, and mechanistic features are obtained for the reaction of **9** with the ethylenic dipolarophile acrylonitrile. Molecular electrostatic potential analyses of the 1,3-dipole and the zwitterionic transition states are found to be very useful for characterizing their electron delocalization features. The solvation effects can enhance the feasibility of these reactions as they stabilize the zwitterionic transition states to a great extent.

### Introduction

1,3-Dipolar cycloaddition reactions are versatile organic transformations, used mainly for the synthesis of a variety of five-membered heterocyclic ring systems.<sup>1–13</sup> In these reactions,

the dipolarophile is normally an alkene/alkyne derivative or a heteroaromatic derivative. In an earlier study, George et al.<sup>14,15</sup>

<sup>#</sup> Dedicated to Professor Dr. Rolf Huisgen, Ludwig-Maximilian Universität, München.

<sup>†</sup> Computational Modeling and Simulation Section, CSIR.

<sup>‡</sup> Photosciences and Photonics Section, CSIR.

<sup>§</sup> Jawaharlal Nehru Centre for Advanced Scientific Research.

(1) Huisgen, R. In *1,3-Dipolar Cycloaddition Chemistry*; Padwa, A., Ed.; John Wiley & Sons: New York, 1984; Vol. 1.

(2) Houk, K. N.; Gonzalez, J.; Li, Y. *Acc. Chem. Res.* **1995**, *28*, 81.

(3) Kobayashi, S.; Jørgensen, K. A. *Cycloaddition Reaction in Organic Synthesis*; Wiley: New York, 2001.

(4) Gothelf, K. V.; Jørgensen, K. A. *Chem. Rev.* **1998**, *98*, 863.

(5) Huisgen, R. *Angew. Chem., Int. Ed. Engl.* **1963**, *2*, 565.

(6) Huisgen, R. *J. Org. Chem.* **1976**, *41*, 403.

(7) Huisgen, R.; Mloston, G.; Langhals, E. *J. Org. Chem.* **1986**, *51*, 4085.

(8) Houk, K. N. In *1,3-Dipolar Cycloaddition Chemistry*; Padwa, A., Ed.; John Wiley & Sons: New York, 1984; Vol. 2.

(9) Ess, D. H.; Houk, K. N. *J. Phys. Chem. A* **2005**, *109*, 9542.

(10) Su, M.-D.; Liao, H.-Y.; Chung, W.-S.; Chu, S.-Y. *J. Org. Chem.* **1999**, *64*, 6710.

(11) Karlsson, S.; Hogberg, H.-E. *Org. Prep. Proc. Int.* **2001**, *22*, 103.

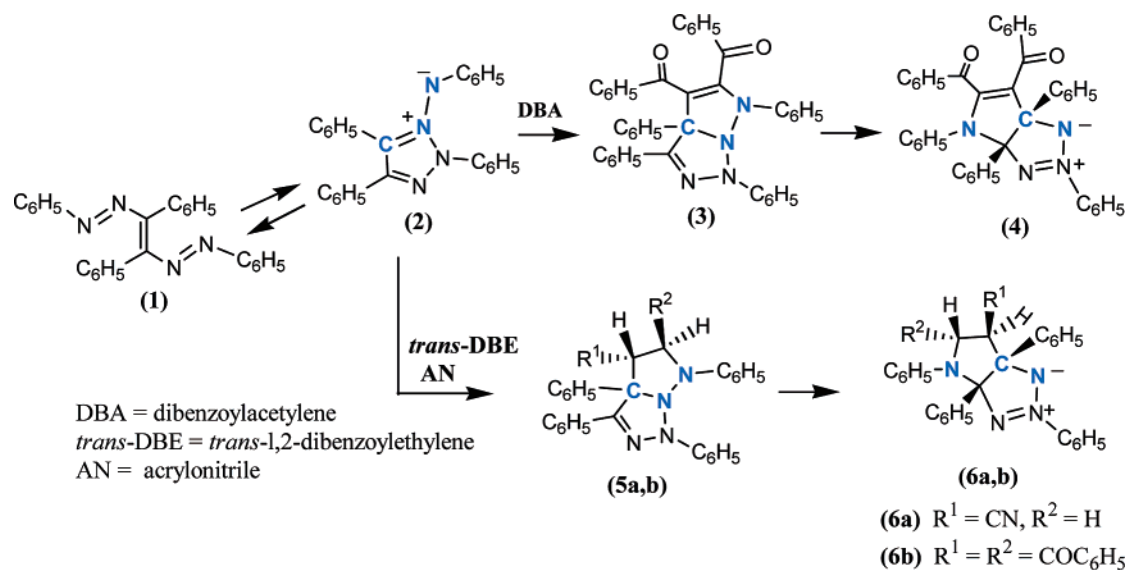
(12) Fisera, L.; Ondrus, V.; Kuban, J.; Micuch, P.; Blanarikova, I.; Jager, V. *J. Heterocycl. Chem.* **2000**, *37*, 551.

(13) Huisgen, R. *Chem. Pharm. Bull.* **2000**, *48*, 757.

(14) Angadiyavar, C. S.; Sukumaran, K. V.; George, M. V. *Tetrahedron Lett.* **1971**, *12*, 633.

(15) Sukumaran, K. V.; Angadiyavar, C. S.; George, M. V. *Tetrahedron* **1972**, *28*, 3987.

## SCHEME 1



have shown that bis(phenylazo)stilbene (**1**) reacts with acetylenic and olefinic dipolarophiles to give the corresponding 1:1 adducts (Scheme 1), arising through a 1,3-dipolar type of cycloaddition. It may be noted that **1** is not a 1,3-dipole. However, it was assumed that an initial pentadienyl anion mode of the cycloaddition of **1** leads to the dipolar form **2** which undergoes further reactions.<sup>16</sup> According to the 2D structure of **2** given in Scheme 1, the 1,3-dipole region of **2** is defined by the three atoms marked in blue (two nitrogen atoms and one carbon atom), and these atoms constitute a zwitterionic triad of atoms with four  $\pi$ -electrons. Thus, the reaction of **1** with dibenzoylacetylene (DBA) was assumed to give the corresponding primary adduct **3**, whereas the reactions of **1** with *trans*-dibenzoyl ethylene (*trans*-DBE) and acrylonitrile were expected to give the corresponding primary adducts **5a** and **5b**, respectively (Scheme 1). However, subsequent X-ray crystallographic analysis had revealed that the adducts were correctly represented by structures **4** and **6a,b**,<sup>17</sup> formed through a facile and unusual rearrangement of the corresponding primary adducts **3** and **5a,b**, respectively (Scheme 1). Subsequent to our initial report on the involvement of bisphenylazoalkenes as potential 1,3-dipolar substrates, Butler et al.<sup>18–22</sup> have extensively investigated the reactions of 1,2,3-triazolium-1-imide 1,3-dipoles and related systems with alkene and alkyne dipolarophiles. They have shown that the initially formed cycloadducts undergo facile sigmatropic rearrangement to give fused pyrrolo[2,3-d]triazoline derivatives.<sup>19,21</sup> Butler and Huisgen have correctly designated these rearrangements as allowed suprafacial thermal 1,4-sigmatropic rearrangements of conjugated organic nitrogen systems, which are analogues of

the 1,5-sigmatropic rearrangement of carbon systems.<sup>20</sup> A key feature of the 1,4-rearrangement is the formation of a single product (product **6** from **5**, Scheme 1), with preservation of the steric arrangement of the substituents  $R^1$  and  $R^2$  on the carbon chain. This implies a process which does not allow for bond rotations during the rearrangement. In a very recent work, Butler et al.<sup>22</sup> have demonstrated that further rearrangement of pyrrolo[2,3-d]triazoline can yield ring-expanded triazine derivatives, and their photonic properties were suggested for potential applications in labeling experiments in biological systems. In the present work, we undertake a theoretical study using the density functional theory (DFT) method to unravel the details of the mechanism of these transformations. We have resorted to the calculations because the DFT methods have been accepted as efficient and reasonably accurate methods, and they have become a powerful tool in molecular modeling, particularly for the ground state properties.<sup>23,24</sup>

## Computational Methods

All of the molecular geometries were optimized at the DFT level by using the Becke's three-parameter exchange functional in conjunction with the Lee–Yang–Parr correlation functional (B3LYP method)<sup>25–27</sup> as implemented in the Gaussian 03 suite of programs.<sup>28</sup> For all the atoms, the 6-31G(d) basis set was selected. For all of the optimized structures, normal coordinate analysis has been performed to characterize them as either minimum or transition state structures. All of the energy minimum structures showed positive eigenvalues of the Hessian matrix, whereas transition states (TSs) showed one negative eigenvalue. For most TSs, the analysis including the visualization of the negative frequency was sufficient to specify the corresponding reaction path. In some cases, intrinsic reaction coordinate (IRC) calculations<sup>29,30</sup> near the TS region followed by geometry optimization of both reactants and products were performed to confirm the connectivity of the TSs. Unscaled vibrational frequencies were used to calculate zero-point energy (ZPE) correction to total energy. The Gibbs free energies were also

(16) George, M. V.; Mitra, A.; Sukumaran, K. B. *Angew. Chem., Int. Ed. Engl.* **1980**, *19*, 973.

(17) Ramaiah, D.; Rath, N. P.; George, M. V. *Acta Crystallogr.* **1998**, *C54*, 872.

(18) Butler, R. N.; Cunningham, D.; Marren, E. G.; McArdle, P. *J. Chem. Soc., Perkin Trans. 1* **1990**, 3321.

(19) Butler, R. N.; Evans, A. M.; Gillian, A. M.; James, J. P.; McNeela, E. M.; Cunningham, D.; McArdle, P. *J. Chem. Soc., Perkin Trans. 1* **1990**, 2537.

(20) Butler, R. N.; Coyne, A. G.; Cunningham, W. J.; Moloney, E. M.; Burke, L. A. *Helv. Chim. Acta* **2005**, *88*, 1626.

(21) Butler, R. N.; Lysaght, F. A.; Burke, L. A. *J. Chem. Soc., Perkin Trans. 2* **1992**, 1103.

(22) Butler, R. N.; Fahy, A. M.; Fox, A.; Stephens, J. C.; McArdle, P.; Cunningham, D.; Ryder, A. *J. Org. Chem.* **2006**, *71*, 5679.

(23) Parr, R. G. *Density-Functional Theory of Atoms and Molecules*; Oxford University Press: New York, 1995.

(24) Seminario, J. M.; Politzer, P. *Modern Density Functional Theory. A Tool for Chemistry*; Elsevier: Amsterdam, 1995.

(25) Becke, A. D. *Phys. Rev. A* **1988**, *38*, 3098.

(26) Becke, A. D. *J. Chem. Phys.* **1993**, *98*, 5648.

(27) Lee, C. T.; Yang, W. T.; Parr, R. G. *Phys. Rev. B* **1988**, *37*, 785.

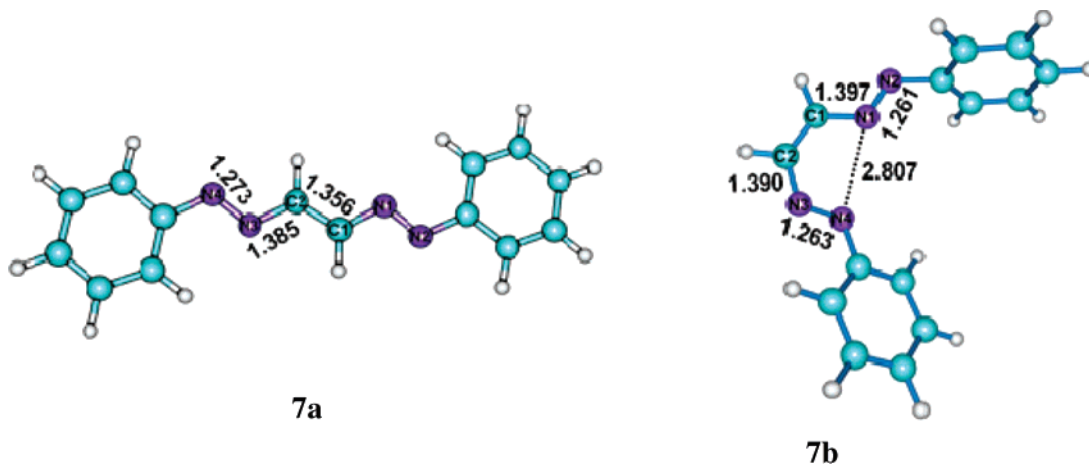


FIGURE 1. Two different isomers of 7 (7a and 7b). All bond lengths in angstrom.

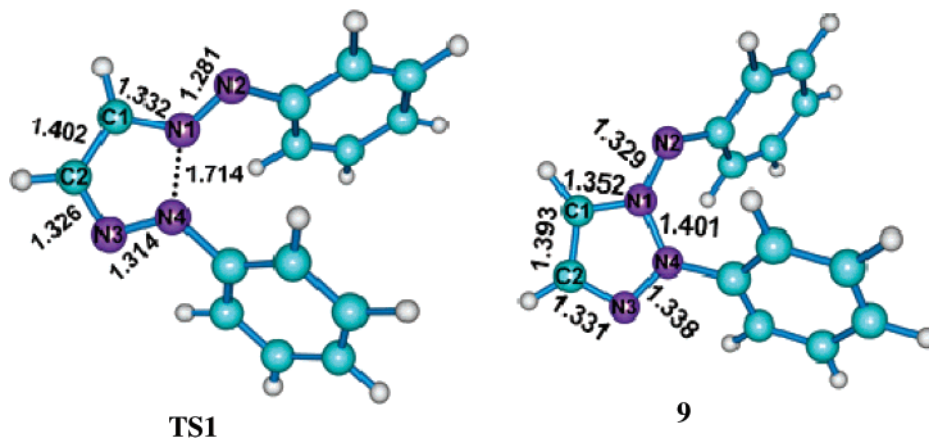


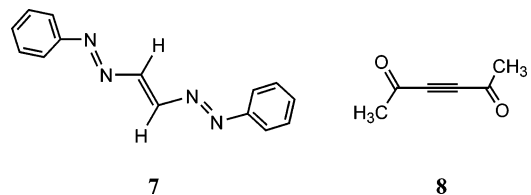
FIGURE 2. Transition state TS1 leading to the formation of the 1,3-dipole system 9. Bond lengths in angstrom.

calculated employing the usual approximations of statistical thermodynamics (ideal gas, harmonic oscillator, and rigid rotor) at the temperature of 298.15 K and the pressure of 1.00 atm. Unless otherwise specified, Gibbs free energy changes are always used for the discussion of energetics. Using the optimized geometries in the gas phase, bulk solvent effects to the activation free energy were calculated via the self-consistent reaction field (SCRF) method, using the Klamt's form<sup>31</sup> of the conductor version of PCM (C-PCM).<sup>32</sup> The atomic charges were computed using Cioslowski's generalized atomic polar tensor (GAPT) method<sup>33</sup> as implemented in Gaussian 03. Further, the molecular electrostatic potential (MESP) was calculated for selected systems at the B3LYP/6-31G-(d) level.<sup>34–38</sup>

In the present work, we have modeled the reaction of **1** with DBA and AN. However, because of the presence of several phenyl moieties in the reactants, the theoretical modeling of the reactions in Scheme 1 is expected to be computationally expensive. Therefore, in order to reduce the computational cost, we have replaced the  $-\text{COC}_6\text{H}_5$  groups in DBA with  $-\text{COCH}_3$  groups. Further, the phenyl groups attached to the ethylenic double bond in **1** are replaced with hydrogen atoms.

## Results and Discussion

(a) **Formation of the 1,3-Dipole System.** In the calculations, the model system bis(phenylazo)ethylene (**7**) is considered in place of bis(phenylazo)stilbene (**1**). The model for the acetylenic dipolarophile is taken as **8**.



Compound **7** can exist in the *trans*-**7a** and the *cis*-**7b** forms, and the optimized geometries of these forms are depicted in Figure 1. The relative free energies calculated for these two

(28) Frisch, M. J.; Trucks, G. W.; Schlegel, H. B.; Scuseria, G. E.; Robb, M. A.; Cheeseman, J. R.; Montgomery, J. A., Jr.; Vreven, T.; Kudin, K. N.; Burant, J. C.; Millam, J. M.; Yengar, S. S.; Tomasi, J.; Barone, V.; Mennucci, B.; Cossi, M.; Scalmani, G.; Rega, N.; Petersson, G. A.; Nakatsuji, H.; Hada, M.; Ehara, M.; Toyota, K.; Fukuda, R.; Hasegawa, J.; Ishida, M.; Nakajima, T.; Honda, Y.; Kitao, O.; Nakai, H.; Klene, M.; Li, X.; Knox, J. E.; Hratchian, H. P.; Cross, J. B.; Bakken, V.; Adamo, C.; Jaramillo, J.; Gomperts, R.; Stratmann, R. E.; Yazyev, O.; Austin, A. J.; Cammi, R.; Pomelli, C.; Ochterski, J. W.; Ayala, P. Y.; Morokuma, K.; Voth, G. A.; Salvador, P.; Dannenberg, J. J.; Zakrzewski, V. G.; Dapprich, S.; Daniels, A. D.; Strain, M. C.; Farkas, O.; Malick, D. K.; Rabuck, A. D.; Raghavachari, K.; Foresman, J. B.; Ortiz, J. V.; Cui, Q.; Baboul, A. G.; Clifford, S.; Cioslowski, J.; Stefanov, B. B.; Liu, G.; Liashenko, A.; Piskorz, P.; Komaromi, I.; Martin, R. L.; Fox, D. J.; Keith, T.; Al-Laham, M. A.; Peng, C. Y.; Nanayakkara, A.; Challacombe, M.; Gill, P. M. W.; Johnson, B.; Chen, W.; Wong, M. W.; Gonzalez, C.; Pople, J. A. *Gaussian 03*; Gaussian, Inc.: Wallingford, CT, 2004.

(29) Fukui, K. *Acc. Chem. Res.* **1981**, *14*, 363.

(30) González, C.; Schlegel, H. B. *J. Chem. Phys.* **1991**, *95*, 5853.

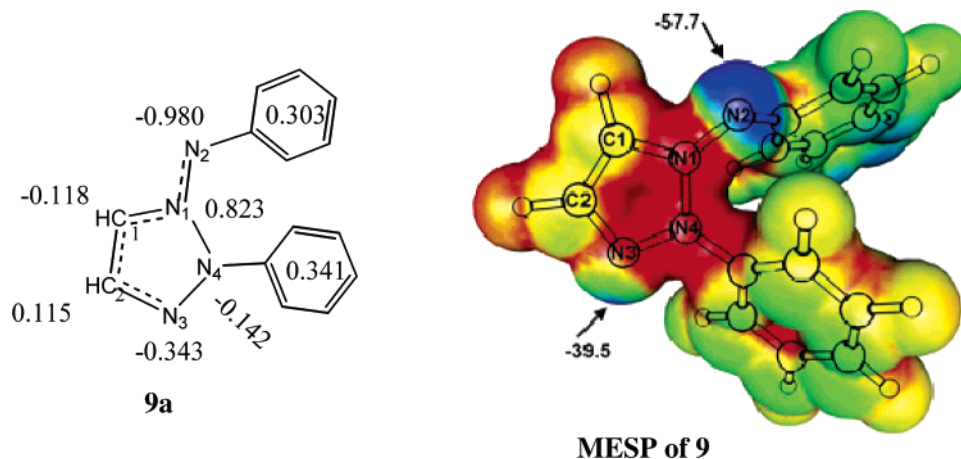


**FIGURE 3.** A schematic structure suitable for **9** with GAP charges (left) and the MESP values plotted on the van der Waals' surface (right). Color coding for red to blue is +62.7 to -25.1 kcal/mol. The most negative-valued MESP points (in kcal/mol) near the N2 and N3 atoms are also marked.

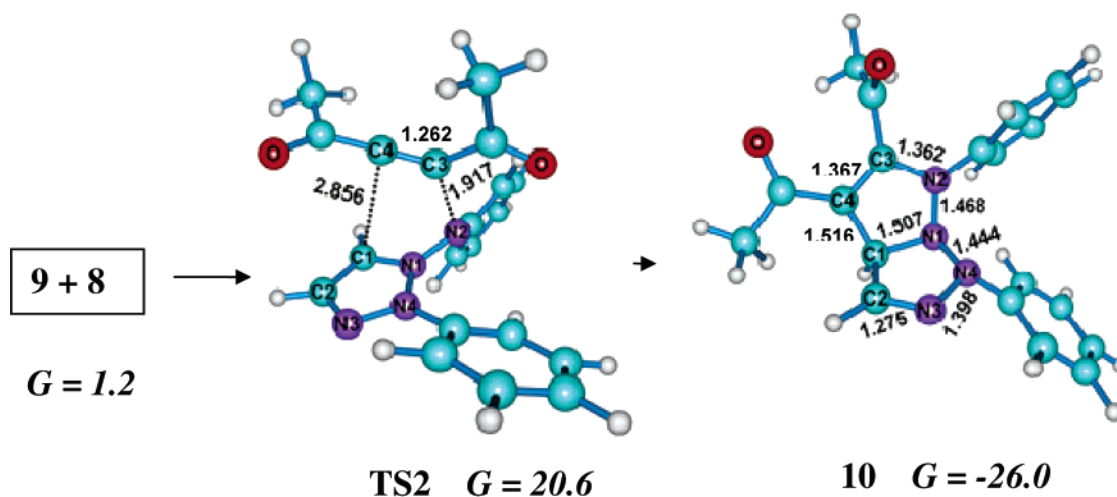


**FIGURE 4.** 1,3-Dipolar cycloaddition between **9** and **8**. All bond lengths in angstrom and relative free energy ( $G$ ) in kcal/mol. Relative free energy of 0.0 kcal/mol is assigned for **7b** + **8**.

forms suggest that **7a** is 2.7 kcal/mol more stable than **7b**. The small amount of destabilization in the *cis*-form can be attributed to the lone pair repulsion from the nitrogen atoms N1 and N4 separated by a distance of 2.807 Å. Although **7b** is less stable than **7a**, the product system **2** given in Scheme 1 can only be obtained from **7b**. Therefore, it is reasonable to assume that, in the experimental reaction conditions, the *trans*-form of bis(phenylazo)stilbene can isomerize to the *cis*-form, and hence we use **7b** as the reactive system for further modeling of the reaction mechanism (see Supporting Information for a possible mechanism for the isomerization of **7a** to **7b**).

In the *cis*-form of bis(phenylazo)ethylene (**7b**), the distance of 2.807 Å found between N1 and N4 atoms suggests the

possibility of a NN bond coupling reaction. A transition state (**TS1**) for NN bond coupling is located, and this led to the formation of the five-membered heterocyclic ring system **9** (Figure 2). The conversion of **7b** to **9** via **TS1** is endergonic by 1.2 kcal/mol, and it requires an activation free energy ( $\Delta G_{\text{act}}$ ) of 5.0 kcal/mol.

A comparison of bond length parameters in **7b** and **9** suggests a drastic electron reorganization in the latter as a result of the newly formed N1–N4 bond. For instance, the N1–C1 (1.352 Å) and N3–C2 (1.331 Å) bonds in **9** are significantly shorter than the corresponding values of 1.397 and 1.390 Å, respectively, found in **7b**. On the other hand, the double bond character of N1–N2 and N3–N4 bonds in **9** is decreased by a considerable extent as they showed an elongation of 0.068 and 0.075 Å, respectively, from the corresponding values in **7b**. These structural features suggest the schematic structure **9a** for **9** wherein the lone pair on N1 is conjugated mainly over all the unsaturated atoms for a  $6\pi$ -electron delocalization (Figure 3).

The bonding features presented in **9a** point toward a partial positive charge on N1 and partial negative charge on N2. The atomic charges computed on the conjugated atoms using

- (31) Eckert, F.; Klamt, A. *AIChE J.* **2002**, *48*, 369.  
 (32) Barone, V.; Cossi, M. *J. Phys. Chem. A* **1998**, *102*, 1995.  
 (33) Cioslowski, J. *J. Am. Chem. Soc.* **1989**, *111*, 8333.  
 (34) Politzer, P.; Truhlar, D. G. *Chemical Applications of Atomic and Molecular Electrostatic Potentials*; Plenum: New York, 1981.  
 (35) Gadre, S. R.; Shirsat, R. N. *Electrostatics of Atoms and Molecules*; Universities Press: Hyderabad, India, 2000.  
 (36) Suresh, C. H.; Gadre, S. R. *J. Am. Chem. Soc.* **1998**, *120*, 7049.  
 (37) Suresh, C. H.; Gadre, S. R. *J. Org. Chem.* **1999**, *64*, 2505.  
 (38) Suresh, C. H. *Inorg. Chem.* **2006**, *45*, 4982.

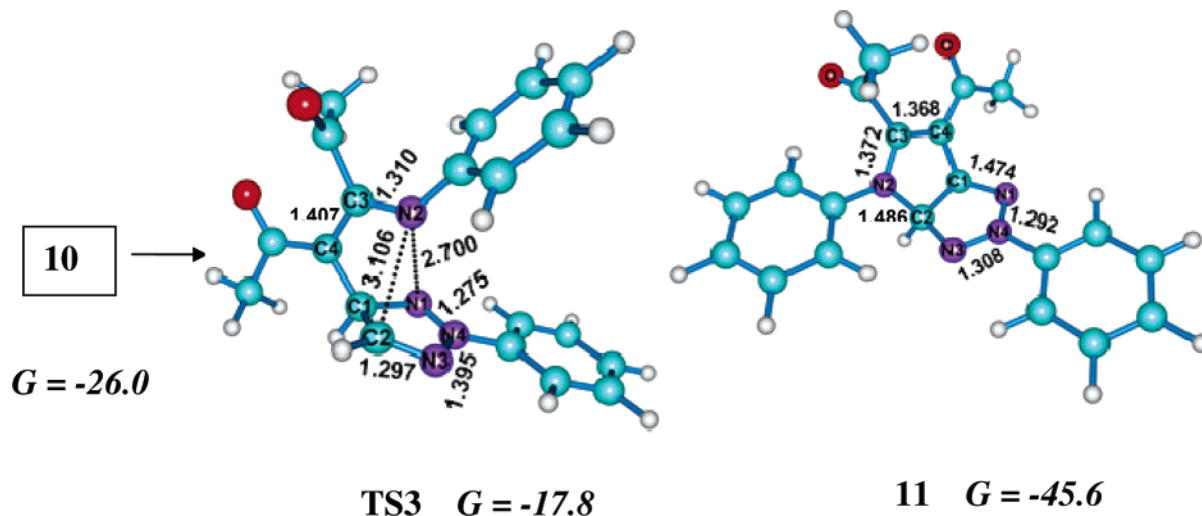


FIGURE 5. Optimized structures of **TS3** and **11**. All bond lengths in angstrom and relative free energy in kcal/mol. Relative free energy of 0.0 kcal/mol is assigned for **7b** + **8**.

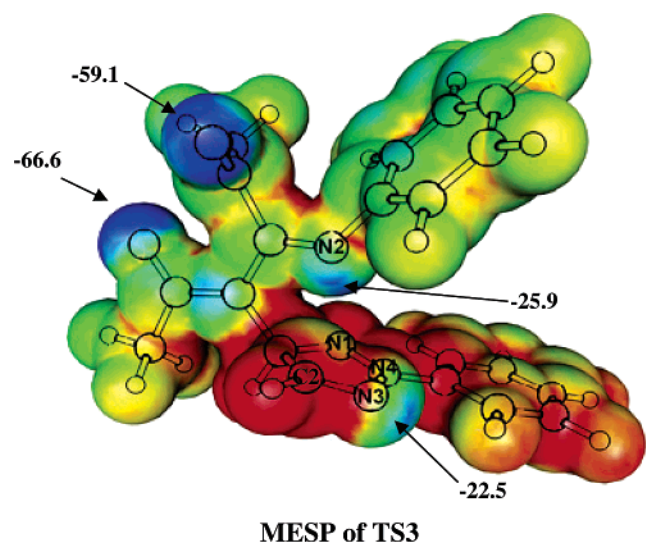


FIGURE 6. MESP plotted onto the van der Waals' surface of **TS3** showing the highly zwitterionic character of the system. Color coding for red to blue is +62.7 to -25.1 kcal/mol. The most negative-valued MESP points (in kcal/mol) are also marked.

Cioslowski's generalized atomic polar tensor (GAPT) method<sup>33</sup> given in **9a** further support the charge separation in N1 and N2 atoms (hydrogen atom values are summed to C1 and C2). The N2 atom is the most negative, while N1 is the most positive. Among the carbon atoms, C1 has significant negative charge. The charge separation seen on the N1–N2 bond is typical of the zwitterionic nature of a 1,3-dipole. Also computed is the molecular electrostatic potential (MESP) values for **9** which reflects the electron-rich and electron-deficient region of the molecule.<sup>34–38</sup> The highest negative valued MESP point (–57.7 kcal/mol) is seen in the lone pair direction of the N2 atom, which supports its high negative charge found in the GAPT population analysis (Figure 3). In other words, a strong nucleophilic character is expected for the N2 atom in its lone pair direction. Similarly, the lone pair direction of the N3 atom also shows a high negative MESP of –39.5 kcal/mol. It may be noted that, in Scheme 1, bis(phenylazo)stilbene (**1**) is presented as a pre-reactant and the active species in the reactions is the five-

membered ring system **2**. The reactivity of **2** can be mainly attributed to the zwitterionic character of the exo N–N bond, and the structural and electronic features obtained for **9** are in good agreement with this argument.

(b) **1,3-Dipolar Cycloaddition.** The 1,3-dipolar cycloaddition involving **9** and **8** (model for DBA) is summarized in Figure 4. In **TS2**, C3...N2 interaction is highly preferred over the C4...C1 interaction, as the former shows a distance of 1.917 Å compared to a distance of 2.856 Å for the latter. The electron-withdrawing acyl substituents in **8** impart electron-deficient character to the acetylenic carbon atoms, and therefore, strong C3...N2 interaction in **TS2** can be considered as resulting from the interaction between highly nucleophilic N2 of **9** with the electron-deficient acetylenic triple bond. Although **TS2** suggests the preferential formation of a C3–N2 bond, the optimization of the product system by following the imaginary frequency of **TS2** results in the simultaneous formation of C3–N2 and C4–C1 bonds yielding the cycloadduct **10**. Therefore, the reaction can be considered as a concerted 1,3-dipolar cycloaddition.<sup>39,40</sup>

The  $\Delta G_{\text{act}}$  for this reaction is found to be 19.4 kcal/mol, and it is exergonic by 27.2 kcal/mol. Thus, the formation of the thermodynamically stable intermediate product **10** explains the formation of the 1,3-dipolar cycloadduct **3** depicted in Scheme 1.<sup>14,15</sup>

(c) **Rearrangement Reactions.** As illustrated in Scheme 1, the reaction did not stop at **3**, and it has further undergone a rearrangement to yield the final product **4**.<sup>17</sup> This step of the reaction is modeled using **10**. The transition state **TS3** is located for the migration of the N2-bearing fragment to the C2 atom in **10**, leading to the formation of the final product **11** (Figure 5). This step of the reaction required only a small  $\Delta G_{\text{act}}$  of 8.2 kcal/mol, and the product **11** was 19.6 kcal/mol more stable than the intermediate product **10**. The thermodynamic driving force for **10** → **11** (as for **3** → **4**) comes from the conversion of a NN into a CN bond and the stabilization energy of the 1,3-dipole in **11**.

Structure of **TS3** is very interesting because, in this transition state, the distance of 2.700 Å between N1 and N2 suggests the

(39) Suser, J.; Sustmann, R. *Angew. Chem., Int. Ed Engl.* **1980**, *19*, 779.

(40) Houk, K. N.; Li, Y.; Evansck, J. D. *Angew. Chem., Int. Ed Engl.* **1992**, *31*, 682.

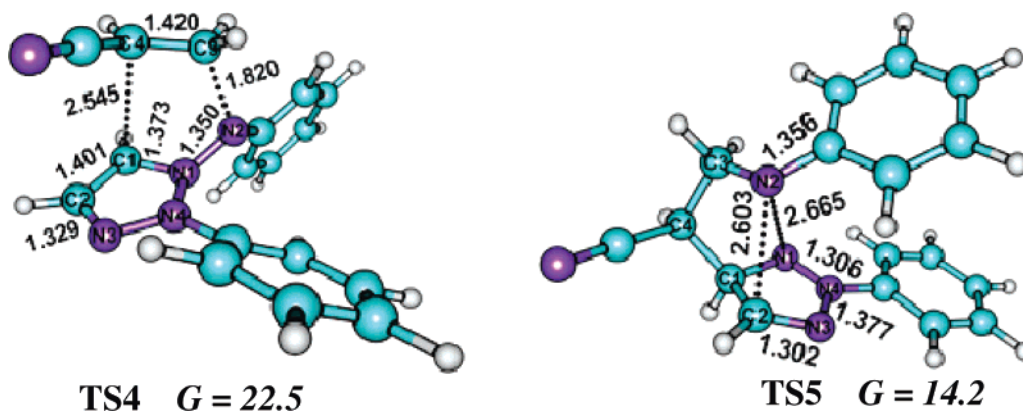
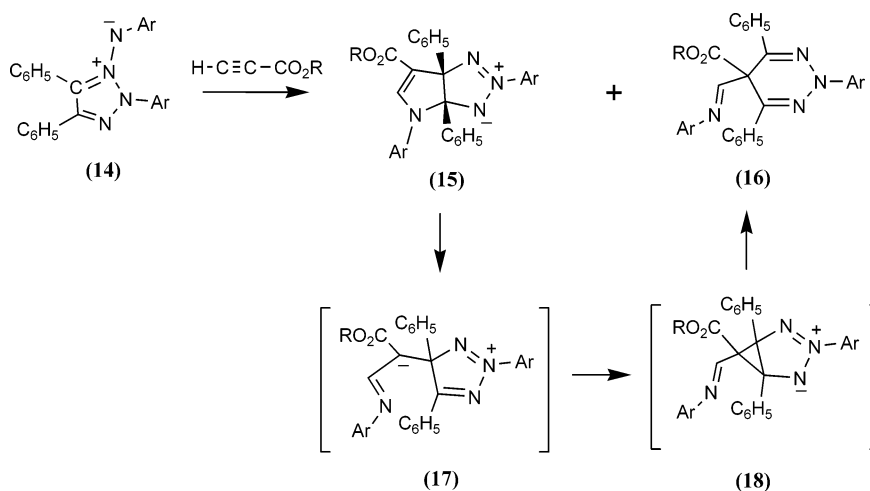


**FIGURE 7.** Optimized structures of **TS4** and **TS5**. The relative free energy with respect to free energy of **7b** + **AN** is also depicted. The relative free energies of **12** and **13** are 0.9 and  $-23.8$  kcal/mol, respectively. All bond lengths in angstrom and relative free energy in kcal/mol.

#### SCHEME 2



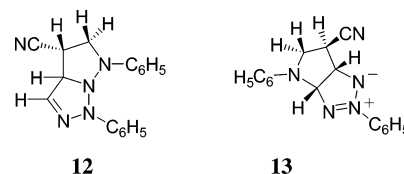
complete rupture of the N1–N2 bond. Further, the bond formation of C2–N2 has also not taken place (C2–N2 distance is 3.106 Å). Considering a typical value of 40 kcal/mol for the N–N single bond strength, the N–N bond breaking in **TS3** suggests a high energy for the transition state. Therefore, the small destabilization of only 8.3 kcal/mol observed in **TS3** indicates additional stabilizing interactions in the system. It may be noted that, in **TS3**, the N1–N4 bond of length 1.275 Å is more like a double bond, which means that the N4 atom having four bonds must bear a positive charge. In other words, the N1–N2 bond breaking takes place in a heterolytic manner, leaving the negative charge on the N2 atom. Therefore, in **TS3**, the negatively charged N2 atom pointing toward the positively charged N4 atom incorporates a stabilizing electrostatic interaction in the system. This could be the probable reason for the high stability of **TS3**.

Further evidence for the electrostatic interaction is obtained from the MESP analysis. In Figure 6, the MESP plotted onto the van der Waals' surface of **TS3** is given, which shows clearly the charge separation in the system. The positive MESP region (red region) is mainly on the five-membered ring containing the N1, N3, and N4 atoms, while the N2 atom migrated to the acetylenic carbon is characterized by the negative MESP (blue region). In other words, the **TS3** can be considered as a system possessing a high degree of zwitterionic character.

The transition state model **TS3** consists of two hydrogen atoms on the five-membered ring and two methyl groups. In

the actual experiment, these hydrogen atoms and the methyl groups are replaced with the phenyl groups. Therefore, the charge-separated structure, such as **TS3**, will be further stabilized in the actual system by the enhanced delocalization of both the positive and negative charges by the additional phenyl groups.

We have also studied the reaction of acrylonitrile (**AN**) with



bis(phenylazo)ethylene. The 1,3-dipolar cycloaddition of **AN** with **9** leading to product **12** (similar to **5a** in Scheme 1) and subsequent nitrogen migration leading to **13** (similar to product system **6a** in Scheme 1) is modeled. The transition state **TS4** for the 1,3-dipolar cycloaddition and the transition state **TS5** for the migration of the nitrogen-bearing fragment are presented in Figure 7.

The 1,3-dipolar cycloaddition of **AN** with **9** is found to be very similar to that of the reaction of the acetylenic dipolarophile **8** with **9**. Like in the case of **TS2**, the C3...N2 interaction in **TS4** is found to be stronger than the C4...C1 interaction. The  $\Delta G_{\text{act}}$  of 22.5 kcal/mol is slightly higher than the value of 19.4

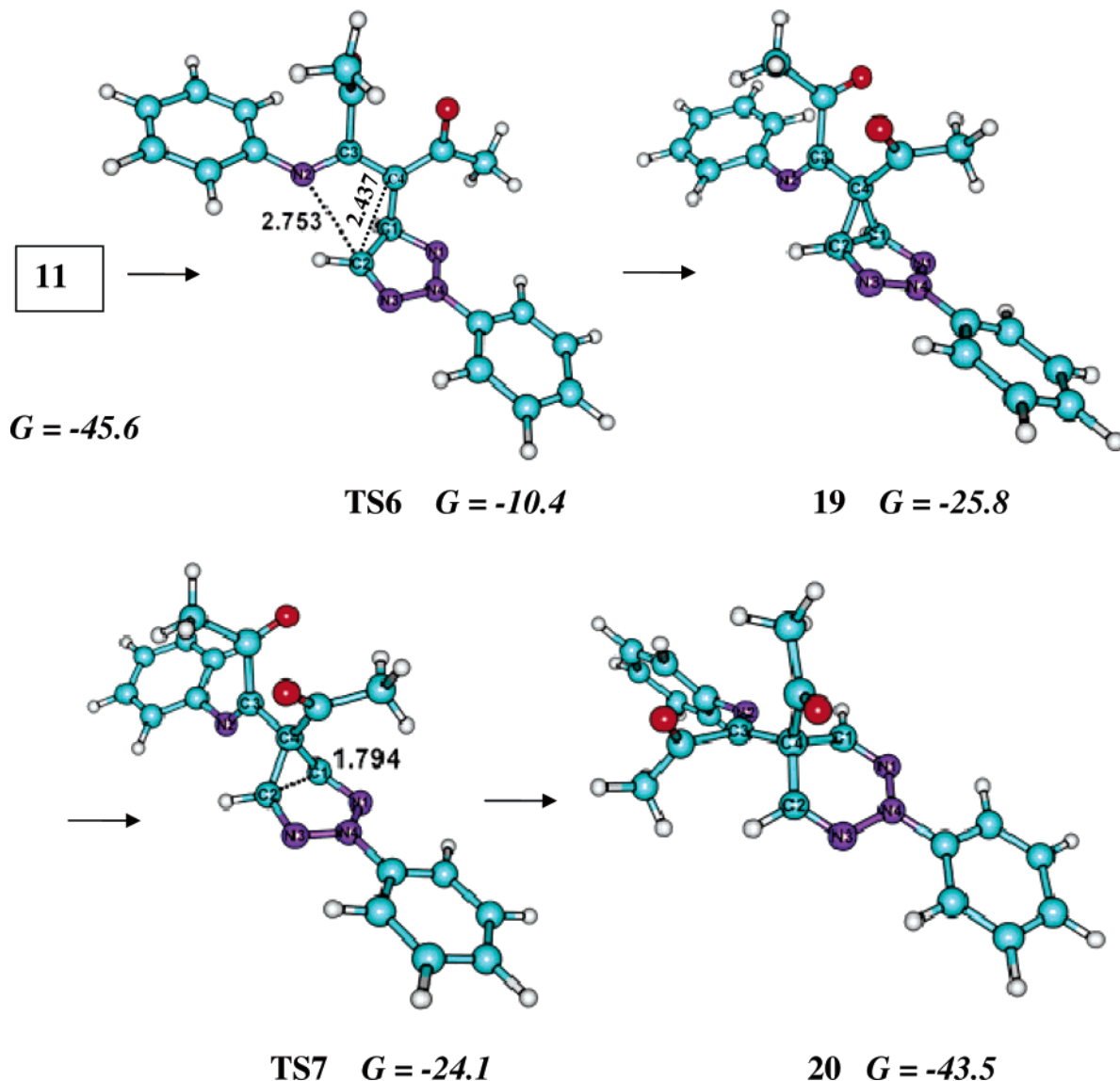


**FIGURE 8.** Activation of the C2–N2 bond in **11** leading to the ring expansion. The relative free energy with respect to **7b** + **8** is given in kcal/mol. All bond lengths in angstrom.

kcal/mol required for the reaction of **8** and **9** (**TS2**). The reaction is a concerted one as **TS4** directly gave the intermediate product **12**.

From **12**, the migration of the nitrogen-bearing fragment occurs through the zwitterionic transition state **TS5**. The structural and electronic features of **TS5** are quite similar to those of **TS3**. The  $\Delta G_{\text{act}}$  of 13.2 kcal/mol obtained from **TS5** is relatively higher than that obtained from **TS3**. The difference in the energetic stabilization of **TS5** and **TS3** can be correlated to their ability to delocalize the zwitterionic charges. The delocalization of the positive charge on the five-membered ring is expected to be the same in both cases. However, in the case of **TS5**, the negative charge on the migrating nitrogen can only be delocalized through the phenyl ring because the other atom connected to that nitrogen atom is an  $\text{sp}^3$ -hybridized carbon atom (C3). On the other hand, in the case of **TS3**, more effective charge delocalization is expected due to the presence of  $\text{sp}^2$ -hybridized C and O atoms.

Although the primary objective of the present work was to establish the mechanism of the reactions given in Scheme 1, the very recent work of Butler et al.<sup>22</sup> suggests that product **11**

in principle can undergo further rearrangement to yield ring-expanded triazine derivatives. They have shown that the reaction of 1,2,3-triazolium-1-aminides (**14**) with propiolate esters, for example, gives rise to a mixture of fused pyrrolo[2,3-d]triazine derivatives (**15**) and 1,2,3-triazine derivatives (**16**), depending on the reaction conditions (Scheme 2).<sup>22</sup> They have suggested that the pyrrolo[2,3-d]triazines (**17**) are the precursors for the triazine derivatives (**16**). The zwitterionic **17** undergoes ring formation to give **18** which subsequently undergoes ring enlargement to give the 1,2,3-triazine derivatives. Similar sequences of reactions have been observed by Butler et al. in the reactions of substituted 1,2,3-triazole 1-oxides with dialkyl acetylene dicarboxylate dipolarophiles.<sup>18</sup> In continuation of the present investigation, we have explored the mechanism of the rearrangement of pyrrolo[2,3-d]triazoles to the corresponding 1,2,3-triazine derivatives using the example of product **11** (Figure 5). The pathway involved in the transformation of **11** to the triazine derivative is indicated in Figure 8.

The transition state **TS6** obtained in this reaction is very similar to the zwitterionic transition state **TS3** located for the migration of the N-bearing fragment. In **TS6**, the C2–N2 bond

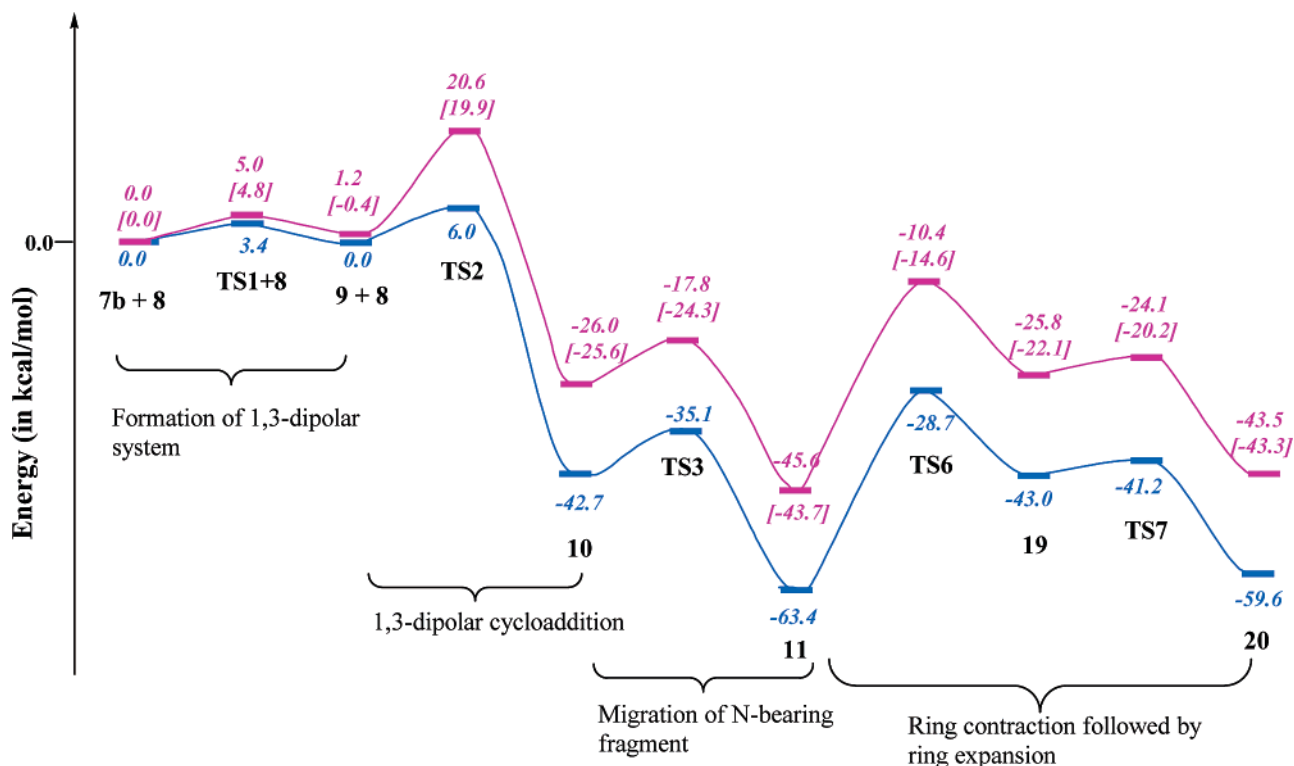


**FIGURE 9.** The relative enthalpy (blue) and relative free energy (pink) profiles (in kcal/mol) in the gas phase. The solvent phase values of relative free energy are given in square brackets.

is completely cleaved, suggesting that its N-bearing fragment has a negative charge while the ring-bearing fragment has positive charge. From **TS6**, the cyclopropyl derivative **19** is formed as a result of a ring contraction reaction involving C2–C4 bond coupling. It means that the cleavage of the C2–N2 bond triggers the simultaneous formation of a C2–C4 bond. A relatively large  $\Delta G_{\text{act}}$  of 35.2 kcal/mol is required for this step. From the intermediate **19**, the cleavage of the C1–C2 bond of the cyclopropyl unit occurs rapidly as it requires only  $\Delta G_{\text{act}} = 1.8$  kcal/mol (**TS7**), leading to the ring expansion product **20**. It may be noted that Butler et al.<sup>22</sup> have used reflux conditions to obtain the ring expansion product, which although supports a high  $\Delta G_{\text{act}}$ , the value of 35.2 kcal/mol obtained for the rate-determining step is not acceptable for a feasible reaction. However, with the use of a full model and the incorporation of the effect of solvation, further reduction in the  $\Delta G_{\text{act}}$  is expected. The effect of solvation will be discussed in the next section.

**(d) Energetics.** The relative enthalpy and relative free energy profiles for the formation of 1,3-dipole system **9** from bis(phenylazo)ethylene, 1,3-dipolar cycloaddition between **9** and dipolarophile **8**, the migration of the N-bearing fragment in the 1,3-cycloadduct, and the ring expansion reaction are presented in Figure 9. Although the activation enthalpy for 1,3-dipolar cycloaddition is only 6.0 kcal/mol, the entropy factor is significant as it raises the activation free energy to 19.4 kcal/mol. Both the 1,3-dipolar cycloaddition and the migration of the N-bearing fragment are highly exothermic processes. Formation of pyrrolo[2,3-d]triazoline derivative **11** is found to be highly exothermic (63.4 kcal/mol) and exergonic (45.6 kcal/mol). From the relative enthalpy change, the migration of the N-bearing fragment (**10** → **TS3** → **11**) appears as the rate-determining step ( $\Delta H_{\text{act}} = 7.6$  kcal/mol) for the formation of **11**. However, in the free energy profile, the highest point **TS2**, observed at 19.4 kcal/mol, suggests that the 1,3-dipolar cy-

cloadduct formation is the rate-determining stage of the reaction. Under drastic conditions, pyrrolo[2,3-d]triazoline may undergo further rearrangement, leading to ring expansion product (1,2,3-triazine derivative).

Also depicted in Figure 9 are the relative values of the free energy in solution computed using the C-PCM method by selecting dichloromethane as the solvent. The free energy of solvation in kcal/mol given in the form of an ordered pair (system, solvation free energy) is (**7b** + **8**, -14.6), (**TS1** + **8**, -14.8), (**9** + **8**, -16.2), (**TS2**, -15.3), (**10**, -14.2), (**TS3**, -21.1), (**11**, -12.7), (**TS6**, -18.8), (**19**, -10.9), (**TS7**, -10.6), and (**20**, -12.4). As we can see, in the solution phase, the zwitterionic transition states **TS3** and **TS6** are more stabilized compared to neutral systems. This in turn decreases the activation free energy from a value of 8.2 kcal/mol in the gas phase to a value of 1.3 kcal/mol in the solution phase for the conversion of **10** to **11**. Similarly, for **11** to **19** conversion, the solvation effect reduces the activation free energy from a value of 35.2 kcal/mol to a value of 29.1 kcal/mol. These results further support the feasibility of the reactions presented in Schemes 1 and 2.

## Conclusions

The model study presented in this work supports a very feasible and highly exothermic reaction of **7** and acetylenic dipolarophile **8** giving the pyrrolo[2,3-d]triazoline derivative **11**. The active species in the reaction is the 1,3-dipole system **9**. The 1,3-dipolar addition occurs in a concerted manner requiring a  $\Delta G_{\text{act}}$  of 19.4 kcal/mol. Since, in the actual reactant species, there are several  $\text{C}_6\text{H}_5$  substituent groups, it is expected that the charge-separated systems similar to **9**, **TS3**, and **TS6** will be further stabilized by the delocalization of the charge via the  $\pi$ -system of the phenyl rings. The 1,3-cycloadduct formed in



the reaction undergoes a very facile rearrangement by a heterolytic N–N bond breaking. The  $\Delta G_{\text{act}}$  for this transformation involving the migration of a N-bearing fragment is found to be 8.3 kcal/mol. The observation of a very clear zwitterionic transition state (**TS3**) is the most characteristic feature of this reaction. Because of the high degree of zwitterionic character of the transition state, charge delocalization through the phenyl rings is found to be very significant in lowering the activation barrier of the nitrogen-bearing fragment. Similar structural, electronic, and mechanistic features are obtained for the reaction of **7** with the ethylenic dipolarophile **AN**. The rearrangement of **11** leading to the expansion of the five-membered ring to a six-membered ring (formation of 1,2,3-triazine derivative) is expected under higher temperatures. This reaction is also characterized by the formation of zwitterionic transition state **TS6** in the rate-determining step. Therefore,  $\pi$ -conjugated substituents in the system are expected to lower the activation barrier. The MESP analysis employed in the present study is

found to be quite useful to characterize the electron delocalization features of the 1,3-dipole and the zwitterionic transition states. The model study presented in this work supports the feasibility of the reactions presented in Scheme 1 as well as the ring expansion reaction recently reported by Butler et al. (Scheme 2).<sup>22</sup>

**Acknowledgment.** We thank the Council of Scientific and Industrial Research, Government of India (C.H.S., D.R., and M.V.G.), and the Jawaharlal Nehru Center for Advanced Scientific Research, Bangalore, India (M.V.G.), for financial support of this work. This is Contribution No. RRLT-PPD-230 from the Regional Research Laboratory, Trivandrum.

**Supporting Information Available:** Optimized geometries and thermodynamic parameters of all the systems. This material is available free of charge via the Internet at <http://pubs.acs.org>.

JO061707S